ELSEVIER

Journal of Archaeological Science 31 (2004) 1215–1224

Journal of Archaeological SCIENCE

http://www.elsevier.com/locate/jas

Calcium–iron–phosphate features in archaeological sediments: characterization through microfocus synchrotron X-ray scattering analyses

W. Paul Adderley[a,*], Ian L. Alberts[b], Ian A. Simpson[a], Timothy J. Wess[c]

[a]*Department of Environmental Science, University of Stirling, Stirling FK9 4LA, Scotland, UK*
[b]*De Novo Pharmaceuticals Ltd, Chivers Way, Histon, Cambridge, CB4 9ZR, UK*
[c]*Structural Biophysics Group, Department of Optometry and Vision Sciences, University of Cardiff, King Edward VII Avenue, Cardiff CF10 3NB, Wales, UK*

Received 30 September 2001; received in revised form 20 November 2001

Abstract

The occurrence of amorphous calcium (Ca)–iron (Fe)–phosphate infilling features in thin-section samples from archaeological stratigraphies is increasingly being reported and used in the cultural interpretations of sites. In some contexts, these materials are the product of dissolution and recrystallization of bone material within pores of the soil or sediment matrix. This study uses transmitted microfocus X-ray scattering to characterize and measure features of known cod fish bone (*Gadus morhua*) materials, and compare them to archaeological samples of amorphous Ca-Fe-phosphate infilling material found in thin section from early fishing community sites. The analyses characterize the structure of these features for the first time, and allow discussion of the diagenetic processes that lead to their formation.

Keywords: Fish bone; Microfocus X-ray small-angle scattering; Diagenesis; Crystal habit; Mineral thickness

1. Introduction

Thin-section micromorphology now has a well-established role in the investigation of archaeological soils and sediments. A key feature of the method is that it provides simultaneous analyses of bioarchaeological and artefactual components, by allowing examination of their spatial relationships at scales of between 10 and 1000 μm. Many advances in the application of the methodology to archaeological contexts have been made, and the technique has been employed in the examination of a wide range of environmental archaeology questions. These include early settlement development [18,21], occupation surfaces in settlement sites [14], and arable agricultural development [4,17,20]. Essential to the understanding and subsequent interpretation of archaeological soil and sediment thin sections is the ability to identify features through microscopic observation. The identification and description of many key features of the matrix material is assisted through recourse to soil and sedimentary literature especially the descriptive handbooks of Bullock et al. [1] and FitzPatrick [5], both based on many years of analyses of agricultural and natural soils. However, many components found in thin sections of archaeological sediments are outside this descriptive arena, in particular bioarchaeological components or 'ecofacts'. Several experimental archaeological studies of specific components have been made where representative source materials are compared. This approach is exemplified by Canti's work on spherulites which has examined both material sources and optical characteristics [2].

One feature that is being increasingly reported in archaeological soil and sediment thin-section studies and used in cultural interpretations of sites is crystalline calcium (Ca)–iron (Fe)–phosphate infilling material,

* Corresponding author. Tel.: +44-1786-467840; fax: +44-1786-467843.
E-mail address: w.p.adderley@stir.ac.uk (W.P. Adderley).

0305-4403/$ - see front matter © 2004 Elsevier Ltd. All rights reserved.
doi:10.1016/j.jas.2002.03.001

found most commonly in moist, temperate and subboreal areas with acidic soil conditions. Jenkins [10], in his analysis of hominid cave sediments at Pontnewydd, North Wales, made the first detailed thin-section analysis of Ca-Fe-phosphate materials in archaeological sediments using microchemical compositional results compared to a variety of mineral types. Jenkins reported orange-brown material coating and infilling voids with a composition approaching that of calcioferrite ($Ca_2Fe_2(PO_4)_3(OH).7(H_2O)$), and concluded that this material had formed following translocation of a discrete Ca-Fe-phosphate colloid derived from bone hydroxyapatite ($Ca_5(PO_4)_3(OH)$). Similar features have also been identified in thin section in a study of early fishing site stratigraphies at Langenesværet, Vesterålen, Northern Norway [19]. This study explored the relationship between medieval commercial fishing stations and earlier fishing activity, demonstrating that medieval commercial fishing settlement was introduced to an area with a long-standing tradition of specialized fishing activity dating from the early centuries AD. Using proton induced X-ray emission (PIXE) spectroscopy, Simpson et al. [19] demonstrated that the yellowish, faintly anisotropic, crystalline infilling materials were Ca-Fe-phosphate features that had their origins as fish bone. Reports of Ca-Fe-phosphate materials have been made in the analysis of thin sections from occupation surfaces found under reduced diagenic conditions [9,13]. Here, these features have been interpreted as being various stages of formation and degradation of vivianite, a similar mode of formation to the isotropic Fe-phosphate material formed under hydromorphic conditions in Belgian bog ore samples [11].

Whilst there is compositional evidence from electron microprobe (e.g. Refs. [9,10]) and from PIXE spectroscopy of these features [19] there are no reported studies of the structural characteristics of this material at the μm scale. In the absence of such studies, understanding of Ca-Fe-phosphate feature formation processes is limited and they remain ambiguous in their interpretation with only limited applicability to broader archaeological questions. In this paper we seek to define the structural characteristics of Ca-Fe-phosphate features derived from fish bone. The methodology adopted to address this is a microfocus X-ray scattering technique used to examine the localized variation in crystal habit from a range of comparative samples: reference fish bone with a variety of pretreatments, and from archaeological Ca-Fe-phosphate infilling material derived from fish bone found at Langenesværet, Northern Norway. The results derived from these analyses are considered in relation to diagenic processes.

1.1. X-Ray scattering methodology

Microfocus X-ray scattering is a powerful non-destructive technique capable of providing important information about the size, habit and arrangement of mineral crystals in tissues such as bone where the crystallite sizes are in the nanometre length scale. Since the technique is capable of probing textural differences in a sample at a micrometre scale resolution, it is suited to in situ analysis of archaeological material in thin section. The technique measures the scattering from the collection of crystals in an X-ray beam and has been used in bone studies since the 1950s to estimate the size of crystallites [3]. Development in the late 1980s of synchrotron microfocus X-ray technology and of more sensitive X-ray detectors has allowed crystallite texture to be analyzed over a micron sized range in thin sections where focal changes in mineral habit may have occurred with time [6,7]. This has a benefit over conventional X-ray scattering or X-ray diffraction analysis where the point to point resolution on a sample is at least two to three orders of magnitude greater.

Sample preparation for X-ray scattering analysis is relatively straightforward and the technique has an advantage over electron microscopy techniques in that the simultaneous measurement of several thousand crystallites at one time is statistically robust [7]. Another advantage is that the measurement of crystal parameters such as orientation, habit and thickness is not dependent on assumptions made about the perfection of the lattice, as is the case in high angle X-ray or electron diffraction. This method therefore is suited to the needs in addressing the characterization of the Ca-Fe-phosphate material. This study has focussed upon the information that this technique provides, the nanoscale size and shape of mineral crystallites.

2. Materials and methods

2.1. Sediment materials

Undisturbed soil samples were obtained in Kubiëna tins from the Vollen site at Langenesværet, Vesterålen, Northern Norway (Fig. 1) [19]. Fig. 2 shows the stratigraphy annotated, and the soil material sampling positions in this profile. Undisturbed blocks of soil materials from Vollen were impregnated with crystic resin. The procedure includes acetone replacement of water in the sample, impregnation by polyester resin, with butan-1-one peroxide catalyst applied under vacuum (Crystic 17449, MEKP; both Scott Bader Ltd.). From these impregnated blocks thin-section samples were prepared in two different ways: (i) glass-mounted and polished thin sections were prepared using standard University of Stirling procedures: cut sections bonded to polished custom slides (110×75×3 mm) using an epoxy system, with mechanical cutting, grinding and polishing (CS10, LP40, PM2A; all Logitech Ltd.) to produce sections of a nominal 30 μm thickness;

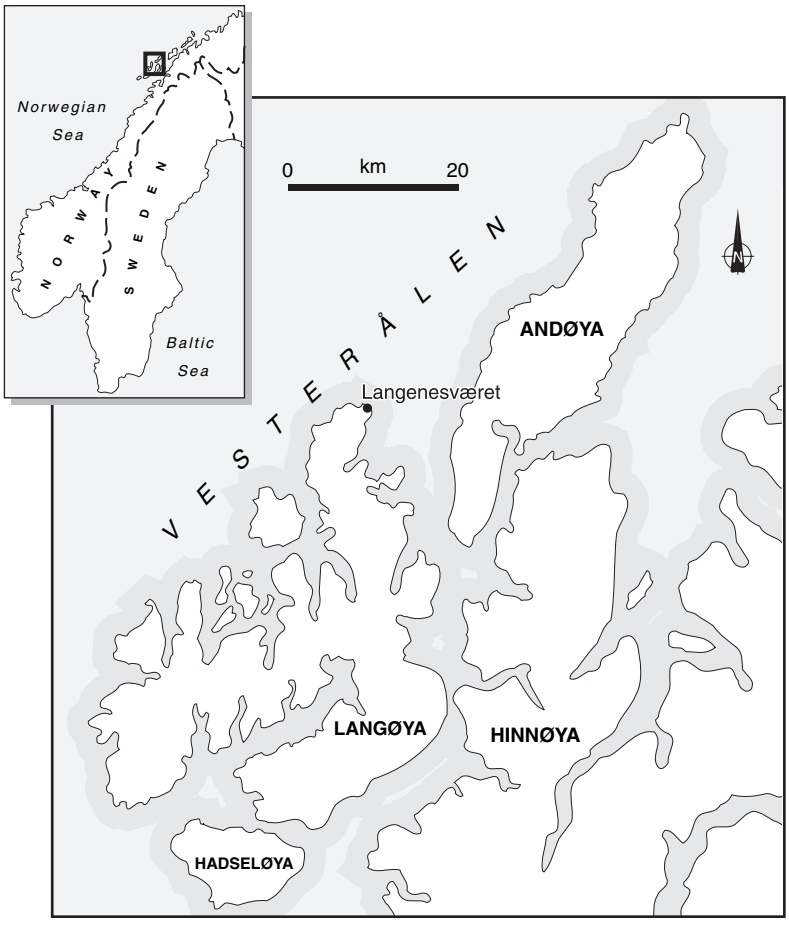

Fig. 1. Map showing location of Langenesværet, Vesterålen, Northern Norway.

(ii) self-supporting 160 μm thick sections (20×20 mm) were cut from the impregnated block using a Buehler (Isomet Low-Speed) sectioning saw with diamond wavering blade, using rapeseed oil (<0.2% water) as a cutting fluid. Using the glass-mounted sections, features were described using the International System [1].

Full thin-section descriptions are provided in Simpson et al. [19], and identify yellowish crystalline infill material. The elemental analysis of these materials by PIXE (Table 1, after Simpson et al. [19]) indicates that the infilling material is rich in Ca, Fe and phosphate relative to other macro-elements, with a high level of strontium indicating a marine origin. The element distribution of these features closely resembles the element distribution of thin-sectioned fish bone material from the same sedimentary sample. The colour characteristics of the materials seen in thin section relate closely to those of the Ca-Fe-phosphate material described by Jenkins [10].

2.2. Reference fish bone materials

Cod (*Gadus morhua*) fish bone was obtained from five fish (19–28 cm in length) caught April 2001 in the River Forth at Kincardine, Scotland. Major parts of the flesh of the fish were removed by dissection, leaving the skeleton intact. This was then further prepared by either (i) boiling vigorously for 30 min with bones wet-sieved (>500 μm) from flesh, or (ii) removing bones from the flesh of fresh fish by dissection. All the bone material obtained was stored frozen until analysis. Materials selected for analysis were the pre-caudal and caudal (tail) vertebrae (Fig. 3).

2.3. Microfocus X-ray scattering

A scheme of the instrumental set-up is shown in Fig. 4. It comprises a small-angle X-ray scattering (SAXS) camera and an imaging facility. Using the unfocussed X-ray beam from the ID22 synchrotron beamline at the ESRF Grenoble, an unfocused, monochromatic beam of 1 mm^2 cross-section was used to illuminate the bone or thin-section sample, mounted on a translation stage for positioning. A high-resolution camera was used to take a radiograph of the sample, which facilitated the identification of micromorphological features in situ. A microbeam of 2 μm vertical by 7 μm horizontal and with a flux of 5×10^9 photons/s at a wavelength (λ) of 0.086 nm

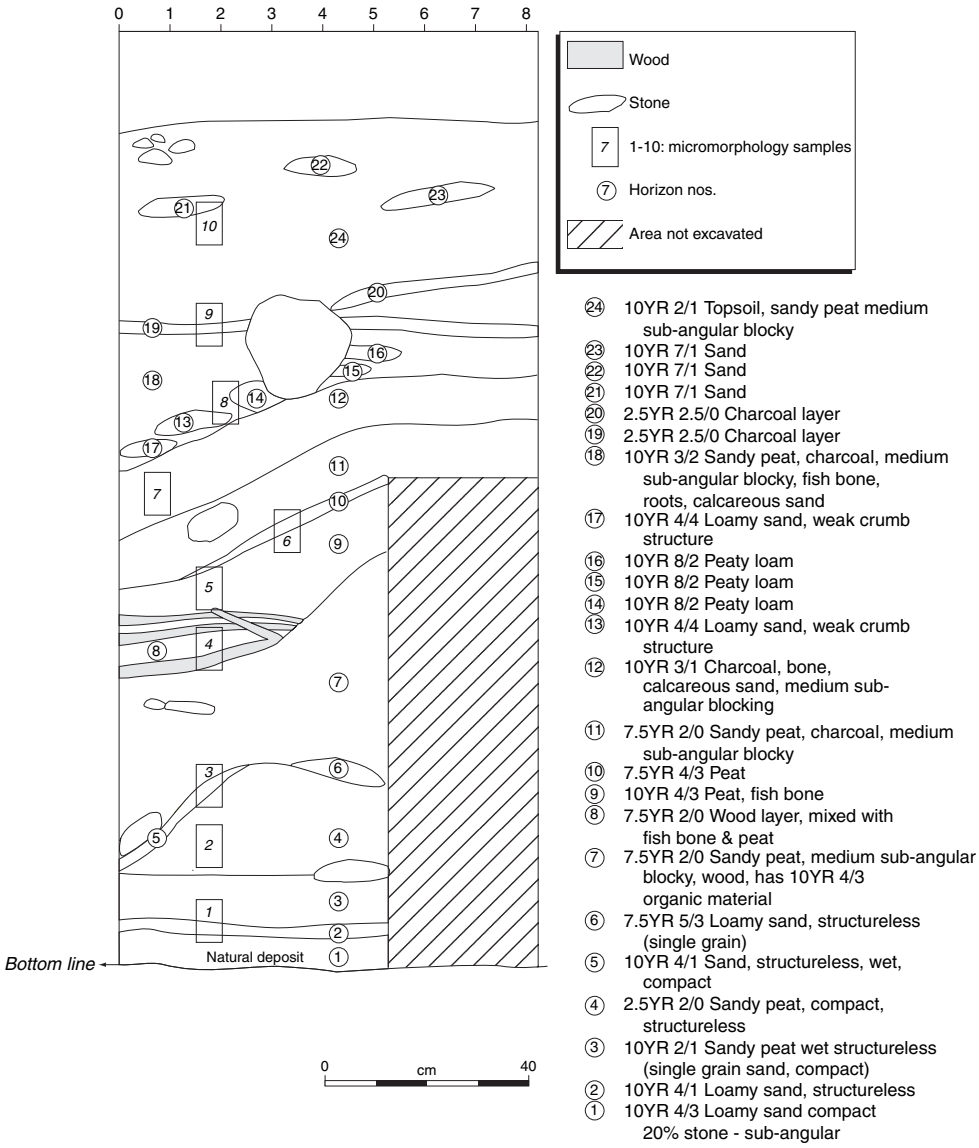

Fig. 2. Profile at Vollen site, Langenesværet annotated with sampling positions and profile stratigraphy.

was generated by positioning the compound refractive lens in the path of the unfocused beam.

Thin-section slides of Ca-Fe-phosphate material were analyzed using microfocus SAXS. Scans at 20 locations were conducted over 400 μm transects (i.e. 20 points at equal intervals). Selected areas within each slide were identified using micromorphological criteria and analyzed.

Table 1
Macro-element PIXE analysis of Ca-Fe-phosphate infilling features of Vollen sample (summarized from Simpson et al., 2000)

Sample (*n*)	Ca (μg/g)	Fe (μg/g)	P (μg/g)	Al (μg/g)	Si (μg/g)
Thin-section fish bone fragment (1)	233541	4683	138285	2525	2158
Ca-Fe-phosphate infilling material (6)					
Mean	50757	17941	35926	8402	8440
Standard deviation	33227	12728	26383	5823	4433
Range					
Maximum	98107	45496	85500	16791	18210
Minimum	15767	7781	5608	2054	5175

2.4. Data treatment

The analysis of X-ray small-angle scattering profiles was conducted using the approach of Fratzl et al. [7] and Wess et al. [22]. Crystal habits such as needles or plates have different characteristic small-angle scattering interactions with X-rays. The size of the crystals also has an effect on the scattering profile. In X-ray scattering, the angular deviation of scatter has an inverse relationship with crystallite size. Therefore, the position and shape of a X-ray scattering curve can be used to derive the average shape and size of crystallites in a sample. Analysis of the

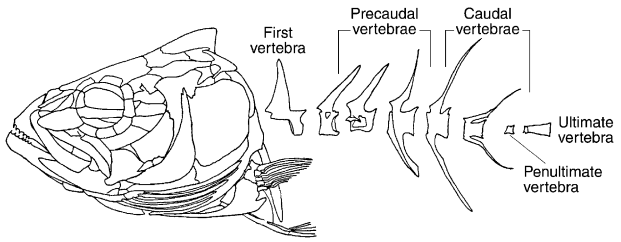

Fig. 3. Fish skeleton components of *Gadus morhua*. Bones used for reference materials were obtained from the abdominal and caudal (tail) vertebrae.

scattering profiles allows two key parameters relating to the habit of crystallites to be measured: the crystal thickness (T) and shape parameter (η).

Multiplying the observed X-ray scattering intensity (I) by the square of the corresponding q value derived from the scattering angle [$q = 2\pi \mathrm{Sin}\theta/\lambda$, where λ is the wavelength of incident X-ray radiation and θ is the scattering angle] gives a Kratky plot ($I(q)q^2$ vs. q) as shown in Fig. 5. Needle- and plate-like crystals give different shaped Kratky plots. In the case of plates, the form factor that corresponds to this shape has an intensity profile that decays by a factor of q^{-2} at values close to $q = 0$. This leads to a flattened region in the Kratky plot at low q values. In the case of a needle crystal habit, the X-ray scattering form factor of this shape has an intensity that decays in proportion to q^{-1} at low q values, leading to a positive slope at low q in the Kratky plot. Since the plot involves the product of I and q^2, the differences in the scattering profiles are enhanced and it is possible to distinguish between these two principal crystal types. A further profile that is observed corresponds to a crystal morphology that is neither representative of needle- nor plate-like crystals. This scattering curve closely matches a Lorentzian distribution and is characteristic of a polydisperse mixture of crystal shapes. This mixture includes large crystals that cannot be studied by small-angle scattering, however, a thickness measurement can still be made for the smaller crystallites.

The thickness parameter T is the average length of the smallest crystal axis. In the case of needle-like crystals,

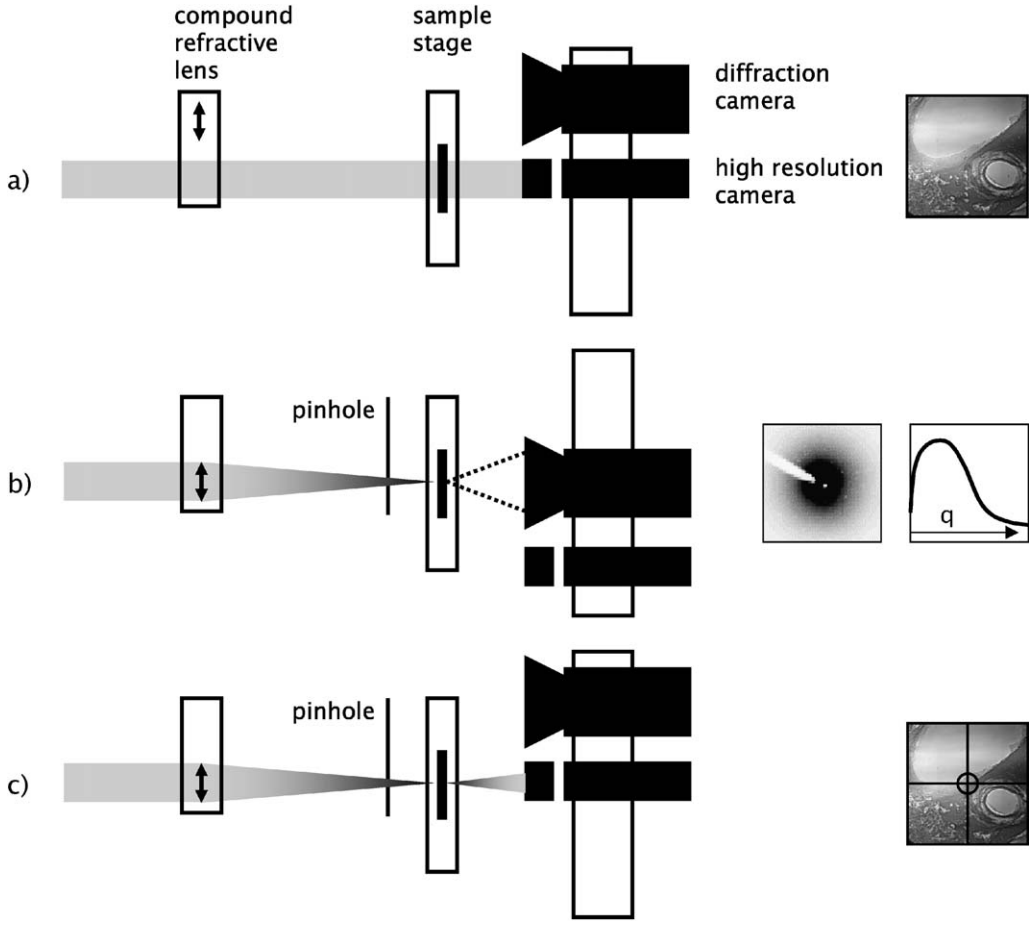

Fig. 4. A schematic diagram of synchrotron microfocus small-angle scattering (SAXS) instrumentation and measurement. The sample radiographic imaging mode is shown in configuration (a) of Fig. 1. The micro-SAXS mode is depicted in configuration (b). A microbeam is created by placing a compound refractive lens (c) in the unfocused beam. A diffraction camera moves into position to record the micro-SAXS pattern. Switching between the two modes takes seconds and provides an effective tool for sample visualization and alignment of the microbeam. An intermediate mode is shown in configuration (c), where the high-resolution camera takes the place of the diffraction camera.

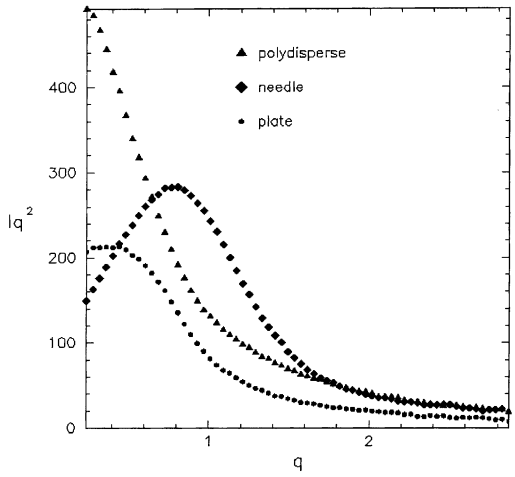

Fig. 5. Kratky plots showing X-ray scattering profiles of different crystallite forms. Scattering profiles that show the representative curves corresponding to different crystallite forms. The data are plotted as the intensity (I) multiplied by q^2, in arbitrary units, against q in nm^{-1}. These profiles show the characteristics for the three main crystalline morphologies: the profile shown as dots is typical of plate-like crystals, the profile shown as diamonds is typical of needle-like crystals, and the profile marked in triangles typifies scattering from polydisperse crystal habits.

either the width or breadth of the crystal corresponds to T. However, in the case of plate-like crystals, T corresponds to breadth, the smallest dimension, since by definition the width of a plate-like crystal is larger than the breadth. The thickness parameter T is defined using the Kratky plot. T is defined as $T = 4K/\pi P$, where K is the integral of the area under the Kratky plot and P is the Porod constant [23]. The Porod constant is derived from the Porod plot [$I(q)q^4$ vs. q^4].

In order to compare differences in shape between scan points, the Kratky plot needs to be rescaled and renormalized to account for different crystallite sizes. The scattering profiles were rescaled by crystal thickness (T) which leads to the definition of a new parameter x, where $x = qT$. These data were then renormalized to give the crystal form factor $G(x)$, such that $\int G(x)\mathrm{d}x = 1$. Plots of $G(x)$ vs. x were superimposed and used to assess the change in the crystal shape. Quantification of the crystal shape was made by comparing the resultant scattering curve to a Lorentzian curve and calculating the residual η, such that $\eta = [G(x) - G_0(x)]^2\mathrm{d}x$, where G_0 is the normalized Lorentzian function $4/[\pi(4+x^2)]$ [7]. Polydisperse crystallites give $G(x)$ vs. x plots that are closer to the Lorentzian function and therefore give lower residual values (η) relative to both plate and needle shaped crystallites.

3. Results and discussion

Fig. 6 shows the position of the 400 μm transect and the 20 scan points examined by SAXS along each

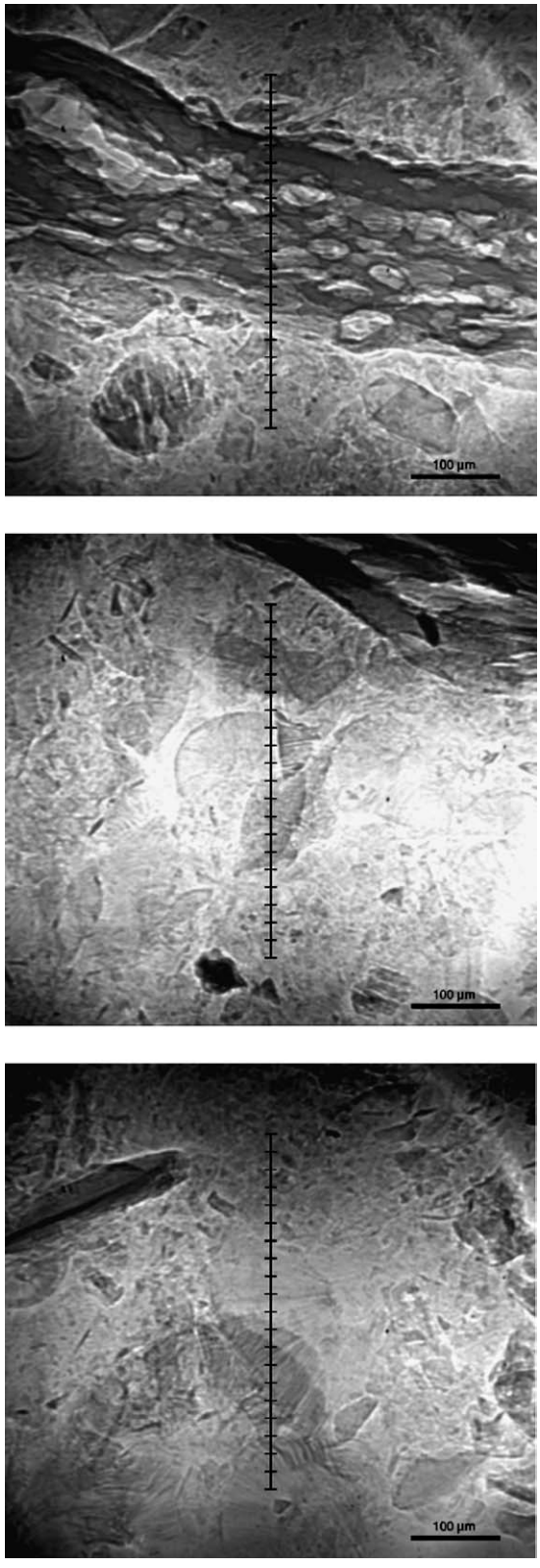

Fig. 6. X-Ray transmission micrographs of Ca-Fe-phosphate features in sediment samples showing microfocus measurement positions. Micrographs were obtained using an unfocussed synchrotron X-ray beam at ESRF beamline ID22. Scan direction: top to bottom. Each transect is 400 μm in length with 20 point measurements made at equal intervals.

transect for thin sections of Ca-Fe-phosphate material. Results from the analysis of the Ca-Fe-phosphate material are presented in Fig. 7. Results of the data analysis for the fish bone reference materials are presented in Fig. 8.

The main parameters that were derived from the study are the crystal thickness parameter (T) and the shape parameter η. The variation of these parameters is shown for three scans in Fig. 7a–c and overlaid scattering functions ($G(x)$) that indicate the variation of crystal form factor in bone are shown in Fig. 7d–f. The average values for T and η are also given, with coefficients of variation (COV) and correlation coefficients in Table 2 for all samples studied. The parameters derived from the control cod bone samples (three points taken from each control sample) are compared with those from the soil sections in order to identify the occurrence of any fish bone in the soil samples and the possible degree of modification.

Scans were conducted in specific regions of several soil sections, where it was judged that remineralization may have occurred. The three scans depicted in the X-ray transmission images in Fig. 6 were the only ones that yielded a significant scattering signal (for example, see Fig. 9). All other scans showed negligible scattering intensity (for example, see Fig. 10). In the three scanned regions, the average crystal thickness values were close to the values measured for the control samples of fresh cod caudal vertebrae (tail) and pre-caudal vertebrae, typically between 2 and 3 nm. The thickness T and shape η parameter values show significant variation (coefficient of variance above 9% for T and above 38% for η), which is perhaps consistent with significant mineral recrystallization. Regions of archaeological and pathological

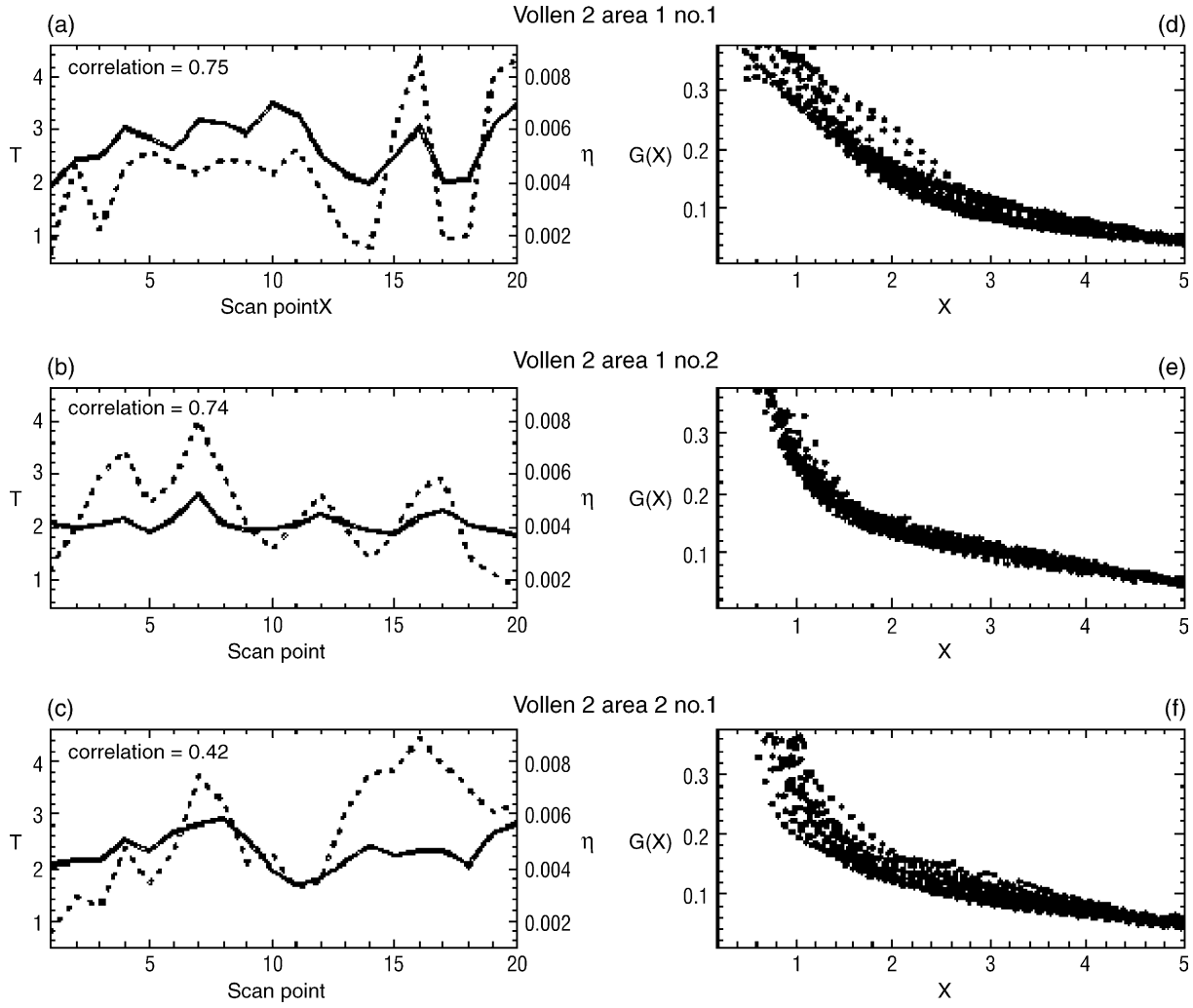

Fig. 7. Crystal habit and form of the thin-section infilling material. Plots a–c show, for each scan point, the variation of the thickness of the crystallites (T) in nm [solid bold line] in comparison with the parameter η in arbitrary units [dotted line] that quantifies the deviation of the crystal shape from a Lorentzian distribution as determined by methods described in the text. Plots d–f represent superimposed $G(x)$ functions that indicate the variation of crystal form factor in the archaeological sediment sample. Plots are shown for three transects as depicted in the X-ray micrographs in Fig. 6.

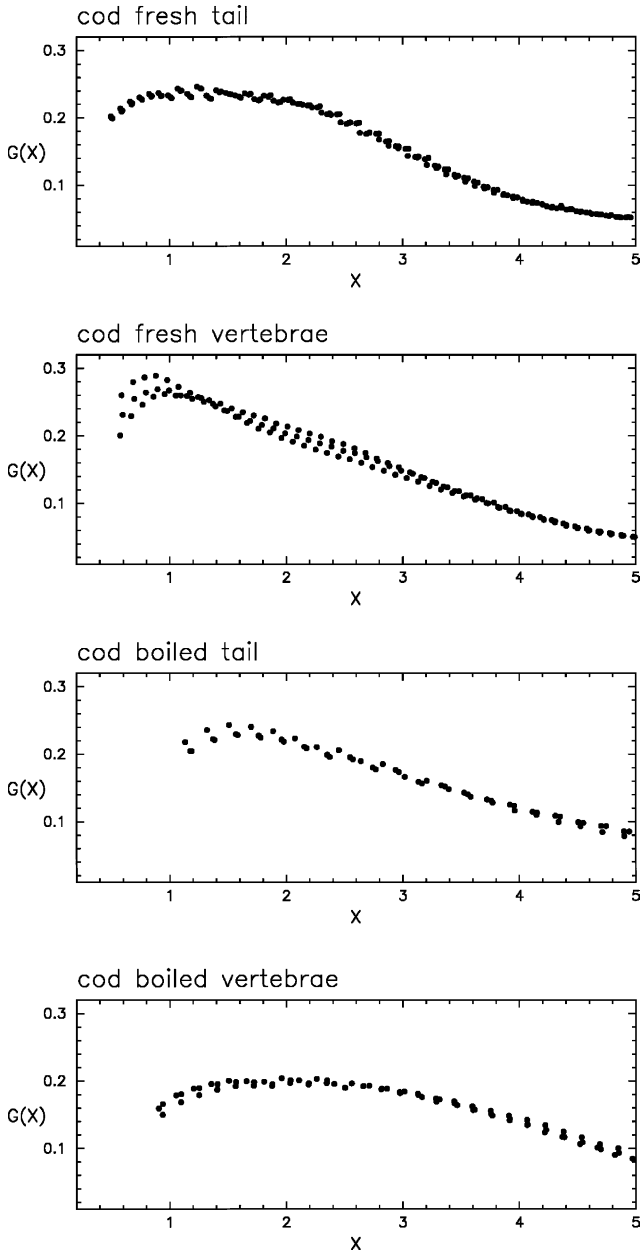

Fig. 8. Superimposed $G(x)$ functions (the form function) that indicate the variation of crystal form factor in bone. Plots are shown for the three points taken from each of the fresh and boiled cod bone samples.

bone containing conspicuous remodelling have previously been shown to exhibit large changes in the T and η parameters [7].

In Fig. 7d–f the scattering profiles of each individual scan are overlaid as form function plots ($G(x)$). This normalizes the effects of crystal size and allows the heterogeneity in the shape of crystallites to be displayed more accurately and gives a good indication as to the deviation of the scattering profile at different points in a scan. It should be noted that the scattering profiles for three points taken from each of the control bone

Table 2
Average parameters for crystallite thickness T (nm) and shape parameter η

Sample	T (nm)	COV (%)	η	COV (%)	CORR
Vollen 2 area 1 no. 1	2.69	18.0	0.0044	51.7	0.75
Vollen 2 area 1 no. 2	2.08	8.55	0.0045	37.7	0.74
Vollen 2 area 2 no. 1	2.32	15.0	0.0054	39.0	0.42
Cod fresh caudal vertebrae (tail)	2.02	1.53	0.0078	6.38	*
Cod fresh pre-caudal vertebrae	2.36	1.95	0.0050	24.8	*
Cod boiled caudal vertebrae (tail)	4.69	2.51	0.0123	0.50	*
Cod boiled pre-caudal vertebrae	3.73	2.18	0.0159	6.57	*

The first column gives the scan number, which relates to the X-ray transmission images shown in Fig. 5. Columns 2 and 3 give the mean crystallite thickness (T in nm) and its coefficient of variance (COV as a % of T). Columns 4 and 5 give the shape parameter (η) and its COV (as a % of η) and the final column gives the linear correlation coefficient between T and η. *Since only three points were taken from each of the fresh and boiled cod samples, a linear correlation coefficient is not statistically significant and is not given.

samples show relatively little divergence indicating that normally, the microstructure of fresh cod bone contains a consistent needle-like crystallite shape (see Fig. 8). This is typical for most modern bones and is in agreement with previous studies by Fratzl et al. [7,8] that showed that the shape parameter is quite highly regulated in normal healthy bone. In contrast, the plots of the three scans in Fig. 7d–f show a polydispersed crystal habit at most points. This is perhaps indicative of bone remodelling through microbial attack in these local regions. A polydispersed crystal habit has been observed previously in regions of bone remodelling in archaeological bone samples [22]. Nielsen-Marsh et al. [16] suggest that there are two diagenetic 'poles' controlled by (rapid) microbial and (slow) chemical degradation of the organic matrix of buried bone, respectively, and mineral diagenesis is believed to be partially governed by the loss of the organic matrix. Whilst the loss of the organic matrix through focal destruction occurs, there will be a slow fossilization of unaltered regions within the bone. It has been contended elsewhere [22] that insights into these chemically-driven diagenetic changes can be obtained from all but the most heavily reworked bone.

The scan in Vollen sample 2 area 1 no. 1 shows the most variation in the T and η parameters (Fig. 7). This can be related to the X-ray transmission image in Fig. 5, which clearly indicates that this scan passes through material of very diverse texture. On either side of the central Ca-Fe-phosphate feature of the image, in points 1 and 15–20 of the scan, the shape function displays a plate-like mineral habit. The development of a variety of crystallite shapes within a single bone sample is likely to be due to the remodelling of bone during the diagenetic process.

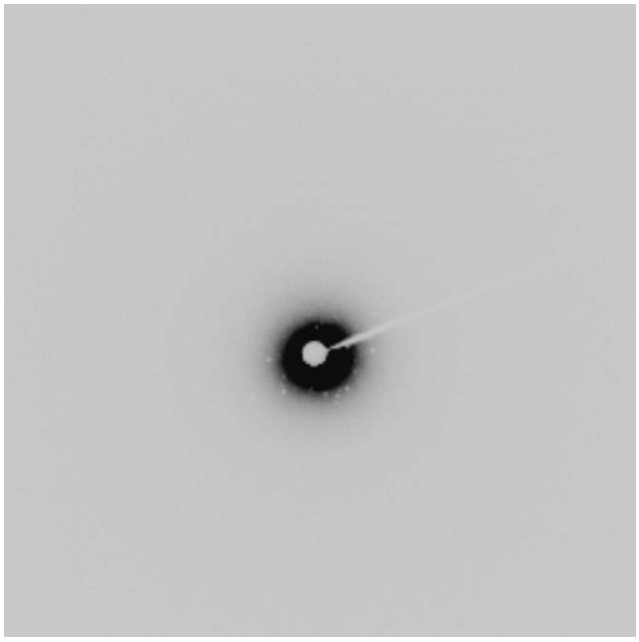

Fig. 9. An example image obtained from crystalline samples showing a strong SAXS signal.

The final column in Table 2 lists the linear correlation (Pearson) coefficients to estimate the association between the thickness and shape parameter values. The profile of the thickness and η plots are qualitatively similar. However, quantitatively, from the values in Table 2, the correlation between these parameters is moderate at best. The correlation is more significant in local regions and may indicate a relationship between crystal shape changes and thickness that could provide a basis for remodelling of fish bone.

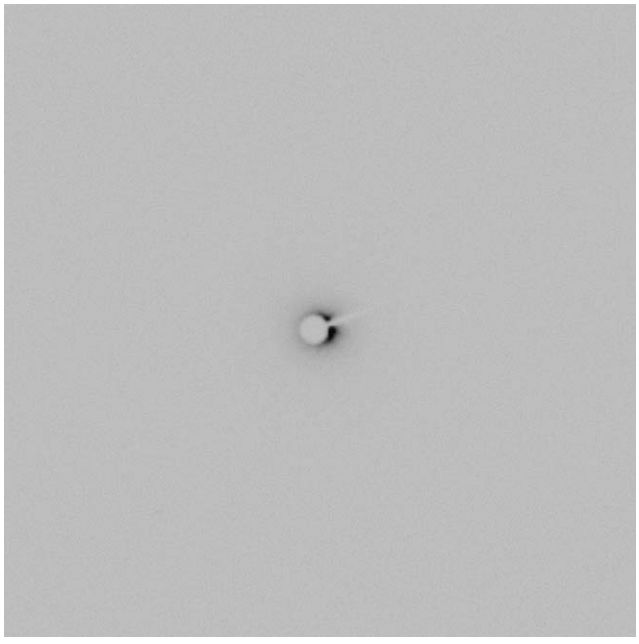

Fig. 10. An example image obtained from samples showing a negligible SAXS signal.

The boiled cod caudal vertebrae (tail) and pre-caudal vertebrae samples also showed a consistent needle-like crystal habit (see Fig. 8). The mean mineral thickness was, however, significantly larger than for the fresh control samples. This increase in T has been observed previously in cooked archaeological bone samples (I.L. Alberts, unpublished data). It indicates that the collagen matrix is an important factor in regulating the size and shape of minerals in bone both in vivo and post-mortem. Pertubations of the collagen structure, altered by treatments such as boiling, allow for the reorganization of mineral. In the soil, the controls for recrystallization of dissolved hydroxyapatite must be presumed to be quite different compared to bone.

4. Conclusion

Both crystalline properties, T and η, of the Ca-Fe-phosphate infilling material, derived using microfocus SAXS, show strong similarities with the reference fish bone material; crystallinity measurements give a strong confirmation that these materials are of fish bone origin, supporting the evidence derived from PIXE analyses. These observations in turn expand the possibilities of interpreting materials found in sites where soil conditions limit conventional zooarchaeological approaches. A further key finding of this work has been to provide an outline of the diagenetic process for the formation of Ca-Fe-phosphate pedofeatures in archaeological soils and sediments. However, the differences found between the boiled and fresh control material samples, and the comparability of Ca-Fe-phosphate material between samples also emphasize the need to further understand diagenetic processes. Studies of the taphonomy and diagenesis of bone materials in archaeological sites have been subject to a wide range of experimental approaches. Chemical characteristics of the burial environment have been considered from a theoretical basis [12] and on the basis of site comparison [15] and it is evident that pH conditions, moisture content and temperature of the burial environment all play major roles in the diagenesis of bone material. A broader set of diagenetic environments in which Ca-Fe-phosphate features are found must be understood and future research should examine the structural formation of these features experimentally under defined and controlled conditions.

Acknowledgements

We would like to thank all the staff at the ESRF Grenoble for help in data collection, especially Michael

Drakopoulos at ID22. The authors wish to thank the Parasitology Group, Institute of Aquaculture, University of Stirling, particularly Drs Andy Shinn and James Bron, for the supply of reference fish material. The Cartography Unit of the Department of Environmental Science, University of Stirling, assisted in the production of the graphics in this paper and George MacLeod produced sample sections of material in the Thin-Section Laboratory.

References

[1] P. Bullock, N. Federoff, A. Jongerius, G. Stoops, T. Tursina, Handbook for Soil Thin Section Description, Waine Research Publications, Wolverhampton, 1985.
[2] M.G. Canti, The micromorphological identification of faecal spherulites from archaeological and modern materials, Journal of Archaeological Science 25 (1998) 435–444.
[3] D. Carlstrom, J.B. Finean, The influence of collagen on the organisation of apatite crystallites on bone, Biochemica et Biophysica Acta 13 (1954) 183–189.
[4] D.A. Davidson, S.P. Carter, Micromorphological evidence of past agricultural practices in cultivated soils: the impact of a traditional agricultural system on soils in Papa Stour, Shetland, Journal of Archaeological Science 25 (1998) 827–838.
[5] E.A. FitzPatrick, Soil Microscopy and Micromorphology, Wiley, Chichester, 1993.
[6] P. Fratzl, N. Fratzl-Zelman, K. Klaushofer, G. Vogl, K. Koller, Nucleation and growth of mineral crystals in bone studied by small-angle X-ray scattering, Calcified Tissue International 48 (1991) 407–413.
[7] P. Fratzl, S. Schreiber, A. Boyde, Characterization of bone mineral crystals in horse radius by small angle X-ray scattering, Calcified Tissue International 58 (1996) 341–346.
[8] P. Fratzl, P. Roschger, J. Eschberger, B. Abendroth, K. Klaushofer, Abnormal bone mineralization after fluoride treatment in osteoporosis: a small-angle X-ray-scattering study, Journal of Bone Mineral Research 9 (1994) 1541–1549.
[9] A. Gebhardt, R. Langhor, Micromorphological study of construction materials and living floors in the medieval motte of Werken (West Flanders, Belgium), Geoarchaeology 14 (1999) 595–620.
[10] D.A. Jenkins, Interpretation of interglacial cave sediments from a hominid site in North Wales: translocation of Ca-Fe-phosphates, in: A.J. Ringrose-Voase, G.S. Humphreys (Eds.), Soil Micromorphology: Studies in Management and Genesis, Elsevier, Amsterdam, 1994, pp. 293–305.
[11] C.J. Landuydt, Micromorphology of iron mineral bog ores of the Belgium Campine, in: L.A. Douglas (Ed.), Soil Micromorphology, a Basic and Applied Science, Developments in Soil Science, 19, Elsevier, Amsterdam, 1990, pp. 289–294.
[12] A.R. Linse, Is bone safe in a shell midden? in: J. Stein (Ed.), Deciphering a Shell Midden, Academic Press, San Diego, CA, 1992, pp. 327–345.
[13] R.I. Macphail, G.M. Cruise, S.J. Mellalieu, R. Niblett, Micromorphological interpretation of a "Turf-filled" funerary shaft at St. Albans, United Kingdom, Geoarchaeology 13 (1998) 617–644.
[14] W. Matthews, C.A.I. French, T. Lawrence, D.F. Cutler, M.K. Jones, Microstratigraphic traces of site formation processes and human activities, World Archaeology 29 (1997) 281–308.
[15] R.A. Nicholson, Fish bone diagenesis in different soils, Archaeofauna 5 (1996) 79–91.
[16] C.M. Nielsen-Marsh, A.M. Gernaey, G. Turner-Walker, R.E.M. Hedges, A.W.G. Pike, M. Collins, The chemical degradation of bone in human osteology, in: M. Cox, S. Mays (Eds.), Archaeology and Forensic Science, Greenwich Medical Media, London, 2000, pp. 439–454.
[17] I.A. Simpson, Relict properties of anthropogenic deep top soils as indicators of infield management in Marwick, West Mainland, Orkney, Journal of Archaeological Science 24 (1997) 365–380.
[18] I.A. Simpson, K.B. Milek, G. Guðmundsson, A reinterpretation of the great pit at Hofstaðir, Iceland using sediment thin section micromorphology, Geoarchaeology 14 (1999) 511–530.
[19] I.A. Simpson, S. Perdikaris, G. Cook, J.L. Campbell, W.J. Teesdale, Cultural sediment analyses and transitions in early fishing activity at Langenesværet, Vesterålen, Northern Norway, Geoarchaeology 15 (2000) 743–763.
[20] M.R. Usai, Textural pedofeatures and pre-Hadrian's Wall ploughed paleosols at Stanwix, Carlisle, Cumbria, UK, Journal of Archaeological Science 28 (2001) 541–553.
[21] G. Wallace, Microscopic views of Swiss Lake Villages, Antiquity 74 (2000) 283–284.
[22] T.J. Wess, I.L. Alberts, J. Hiller, M. Drakopoulos, A.T. Chamberlain, M. Collins, Microfocus small angle X-ray scattering reveals structural features in archaeological bone samples: detection of changes in bone mineral habit and size, Calcified Tissue International 70 (2002) 103–110.
[23] A. Guinier, X-ray diffraction, in: Crystals, imperfect crystals, and amorphous bodies, W.H. Freeman and Co., San Francisco, 1963.